Correlations between electrochemical behaviors and DNA photooxidative properties of non-steroïdal anti-inflammatory drugs and their photoproducts

Sandra Michaud, Viviane Hajj, Laure Latapie, Arielle Noirot, Valérie Sartor, Paul-Louis Fabre, Nadia Chouini-Lalanne

Correlations between electrochemical behaviors and DNA photooxidative properties of non-steroïdal anti-inflammatory drugs and their photoproducts

Sandra Michaud [a,b], Viviane Hajj [a,b], Laure Latapie [c,d], Arielle Noirot [a,b], Valérie Sartor [a,b], Paul-Louis Fabre [c,d], Nadia Chouini-Lalanne [a,b,*]

[a] Université de Toulouse, Université Paul Sabatier, Laboratoire IMRCP, Bat. 2 R1, 118 route de Narbonne, F-31062 Toulouse cedex 09, France
[b] CNRS, Laboratoire IMRCP UMR 5623, F-31062 Toulouse cedex 09, France
[c] Université de Toulouse, Université Paul Sabatier, Laboratoire de Génie Chimique, Bat. 2 R1, 118 route de Narbonne, F-31062 Toulouse cedex 09, France
[d] CNRS, Laboratoire de Génie Chimique UMR 5503, F-31062 Toulouse cedex 09, France

A B S T R A C T

Alkali-labile lesion to DNA photosensitized, *via* an electron transfer mechanism, by three non-steroidal anti-inflammatory drugs (NSAIDs), ketoprofen, tiaprofenic acid and naproxen and their photoproducts during drug photolysis, was investigated using ^{32}P-end labelled synthetic oligonucleotide. These photooxidative damages were correlated with the photophysical and electrochemical properties of drugs, appearing as the photosensitizer PS. Photophysical studies provided the excited state energies of the photosensitizer while their redox potentials and the relative stabilities of the $PS^{\cdot-}$ radical-anions were determined by cyclic voltammetry. On the basis of these data, we have calculated the Gibbs energy of photoinduced electron-transfer and evaluated the exergonicity of the oxidative photodamage. Moreover, kinetic control may be invoked according to the stabilities of $PS^{\cdot-}$. Applied to this NSAIDs family, the photoxidative damages through electron transfer mechanism were analyzed and a good correlation with photoredox and photobiological properties was established.

1. Introduction

Ketoprofen (KP), tiaprofenic acid (TP) and naproxen (NP) (Scheme 1) are non-steroidal anti-inflammatory drugs (NSAIDs) and belong to the arylpropionic acid family. They are amongst the most widely prescribed drugs in the treatment of inflammation and pain. Nevertheless, a side effect associated with this group of drugs is their potential to induce photosensitivity reactions [1,2] that generally involved drug-photosensitized damages to biomolecules. Upon UV radiation, their *in vitro* photosensitizing properties towards cell membranes or DNA have been widely investigated [3,4]. In the case of DNA, photosensitized reactions can take place through different mechanisms. Energy transfer from the triplet state of the photosensitizer (PS^*) to the pyrimidine bases leads to the formation of cyclobutane pyrimidine dimers. Their photosensitization has been reported for KP, TP and NP during drug photolysis [5–8]. Another major source of DNA damage upon exposure to UV radiation is the photosensitized oxidation [9]. These processes may result from a Type I radical mechanism involving the generation of radicals (e.g., via electron transfer or hydrogen abstraction) and/or a Type II mechanism going through the production of singlet oxygen [10]. It has been established that KP, TP and NP photoinduce oxidative DNA damage *via* Type I and/or Type II mechanisms [6–8,11–13].

The photochemistry of these three drugs, centered on the arylpropionic chain, has been extensively studied. In neutral aqueous medium, their photolysis gives three major photoproducts: ethyl, hydroxyethyl and acetyl derivatives (Scheme 1) [14–16].

As each photoproduct bears the parent drug chromophore in its structure, it must be a potential photosensitizer. Photosensitization of lesions by drug photoproducts has been poorly investigated while it is clear that understanding the reactions involved in photobiological processes requires the knowledge of the photophysical properties of the parent drug but also of the photoproducts. Such a study becomes fundamental in the case of photochemically unstable drugs. Indeed, it has been previously demonstrated that the photosensitizing properties of KP and other benzophenone derivatives in DNA depend mainly on the benzophenone chromophore [8]. The involvement of photoproducts in DNA photosensitization processes was already reported for some NSAIDs [17–19]. From a chemical point of view, the alkali-labile lesion to DNA photosensitized, *via* an electron transfer mechanism, appears to be a redox reaction between DNA and the excited state of the photosensitizer. In order to quantify this reaction, electrochemical and photophysical studies could lead to the determination of the redox potential

* Corresponding author at: Université de Toulouse, Université Paul Sabatier, Laboratoire IMRCP, Bat. 2 R1, 118 route de Narbonne, F-31062 Toulouse cedex 09, France.
E-mail address: lalanne@chimie.ups-tlse.fr (N. Chouini-Lalanne).

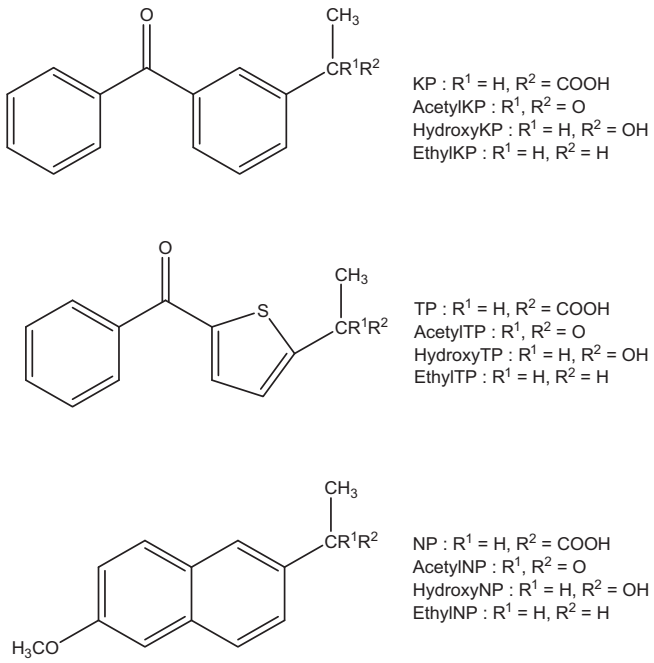

Scheme 1. Chemical structures of ketoprofen (KP), tiaprofenic acid (TP), naproxen (NP) and their major photoproducts.

involving the excited photosensitizer (PS^*). Then, through the Rehm–Weller's equation [20], the exergonicity of the photoxidative damage could be evaluated.

The aim of this paper is to quantify the electron transfer ability of three non-steroidal anti-inflammatory drugs, ketoprofen, tiaprofenic acid and naproxen and their photoproducts towards DNA. For this purpose, their ability to photoinduce DNA alkali labile lesions *via* an electron transfer mechanism were investigated and correlated to their photophysical properties and their electrochemical behaviors.

2. Materials and methods

2.1. Chemicals and biochemical

Ketoprofen, KP (2-(3-Benzoylphenyl) propionic acid) and Naproxen, NP ((*S*)-(+)-2-(6-Methoxy-2-naphthyl)propionic acid) were purchased from Sigma-Aldrich (St Quentin Fallavier, France). Tiaprofenic acid, TP (2-(5-[2-benzoyl]thienyl)propionic acid) was extracted from Flanid (Pierre Fabre medicament production, Boulogne, France). [γ^{32}P] ATP (3000 Ci/mmol), Ready-to-Go T4 Polynucleotide Kinase, and G-25 Microspin columns were from Amersham Pharmacia Biotech (Saclay, France), and piperidine from Acros Organics France (France). Oligonucleotide **1** and its complementary strand **2** were synthesized and purified by polyacrylamide gel electrophoresis by Genosys (UK): oligonucleotide **1**: 5′-TGATC GGTGCGTCTGAGACT-3′.

2.2. Photolysis experiments and isolation of photoproducts

2.2.1. Ketoprofen

Phosphate buffer solutions of KP (10^{-3} mol L^{-1}) were exposed to sunlight until the drug had been totally consumed. HPLC analysis of the irradiated mixture was then performed on a reverse phase column Xterra 3.5 μm (2.1 × 150 mm column) eluted with a gradient of H_2O:CH_3CN (57:43–0:100 over 15 min, to 57:43 over 1 min, isocratic at 57:43 for 19 min; flow rate = 300 μL min^{-1}). The eluate was monitored by following the absorbance at 227 nm with a Waters UV detector and analyzed by MS desorption chemical ionization/NH_3 using TSQ-700 Thermoelectron spectrometer in CH_2Cl_2. The residue was purified by chromatography column (silica gel: Kieselgel 60, 0.063–0.200 mm) using 100% dichloromethane and a mixture of dichloromethane and ethyl acetate (90:10).

2.2.1.1. 3-Ethylbenzophenone (EthylKP). ^{1}H NMR ($CDCl_3$) δ ppm = 7.77–7.30 (m, 9H); 2.67 (q, 2H, *J* = 7.6 Hz); 1.22 (*t*, 3H, *J* = 7.6 Hz). MS: *m*/*z* (uma) = 210; 211 $(M+H)^+$; 228 $(M+NH_4)^+$. UV: λ_{max} (diethyl oxyde) = 252 nm; λ_{max} (ethanol) = 256 nm; λ_{max} (phosphate buffer) = 260 nm.

2.2.1.2. 3-(1-Hydroxyethyl)benzophenone (HydroxyKP). ^{1}H NMR ($CDCl_3$): δ ppm = 7.76–7.38 (m, 9H); 4.93 (*q*, 1H, *J* = 6.6 Hz); 1.70 (s, 1H); 1.48 (*d*, 3H, *J* = 6.5 Hz). MS: *m*/*z* (uma) = 226; 227 $(M+H)^+$. UV: λ_{max} (diethyl oxyde) = 252 nm; λ_{max} (ethanol) = 256 nm; λ_{max} (phosphate buffer) = 260 nm.

2.2.1.3. 3-Acetylbenzophenone (AcetylKP). ^{1}H NMR ($CDCl_3$): δ ppm = 8.31–7.43 (m, 9H); 2.60 (s, 3H). MS: *m*/*z* (uma) = 224; 242 $(M+NH_4)^+$. UV: λ_{max} (diethyl oxyde) = 250 nm; λ_{max} (ethanol) = 252 nm; λ_{max} (phosphate buffer) = 254 nm.

2.2.2. Tiaprofenic acid

Photolysis was performed with the procedure described above. A different gradient of H_2O:CH_3CN (67:33–0:100 over 25 min, to 67:33 over 1 min, isocratic at 67:33 for 19 min; flow rate = 300 - μL min^{-1}) was used for HPLC analysis. The residue was purified by chromatography column (silica gel: Kieselgel 60, 0.063–0.200 mm) using 100% chloroform.

2.2.2.1. 2-Benzoyl-5-ethylthiophene (EthylTP). ^{1}H NMR ($CDCl_3$): δ ppm = 7.80–6.80 (m, 7H); 2.86 (q, 2H, *J* = 7.2 Hz); 1.31 (t, 3H, *J* = 7.2 Hz). MS: *m*/*z* (uma) = 216; 217 $(M+H)^+$; 234 $(M+NH_4)^+$; 251 $(M+N_2H_7)^+$. UV: λ_{max} (diethyl oxyde) = 258 and 302 nm; λ_{max} (ethanol) = 262 and 308 nm; λ_{max} (phosphate buffer) = 266 and 314 nm.

2.2.2.2. 2-Benzoyl-5-(1-hydroxyethyl)thiophene (HydroxyTP). ^{1}H NMR ($CDCl_3$): δ ppm = 7.83-6.75 (m, 7H); 4.68 (q, 1H, *J* = 7.2 Hz); 1.90 (s, 1H), 1.50 (d, 3H, *J* = 7.2 Hz). MS: *m*/*z* (uma) = 232; 250 $(M+NH_4)^+$. UV: λ_{max} (diethyl oxyde) = 258 and 302 nm; λ_{max} (ethanol) = 262 and 308 nm; λ_{max} (phosphate buffer) = 266 and 314 nm.

2.2.2.3. 2-Benzoyl-5-acetylthiophene (AcetylTP). ^{1}H RMN ($CDCl_3$): δ ppm = 7.87–7.43 (m, 7H); 2.57 (s, 3H). MS: *m*/*z* (uma) = 230; 248 $(M+NH_4)^+$, 265 $(M+N_2H_7)^+$. UV: λ_{max} (diethyl oxyde) = 300 nm; λ_{max} (ethanol) = 304 nm; λ_{max} (phosphate buffer) = 310 nm.

2.2.3. Naproxen

Photolysis was performed with the procedure described for KP. The residue was purified by chromatography column (silica gel: Kieselgel 60, 0.063–0.200 mm) using 100% chloroform and a mixture of dichloromethane and ethyl acetate (98:2).

2.2.3.1. 2-Ethyl-6-methoxynaphtalene (EthylNP). ^{1}H NMR ($CDCl_3$): λ ppm = 7.64–7.11 (m, 6H); 3.34 (s, 3H); 2.73 (q, 2H, *J* = 7.2 Hz); 1.52 (t, 3H, *J* = 7.4 Hz). MS: *m*/*z* (uma) = 186; 204 $(M+NH_4)^+$. UV: λ_{max} (diethyl oxide) = 232, 264, 272, 318 and 334 nm; λ_{max} (ethanol) = 232, 262, 272, 318 and 332 nm; λ_{max} (phosphate buffer) = 226, 264, 276, 314 and 332 nm.

2.2.3.2. 2-(1-Hydroxyethyl)-6-methoxynaphtalene (HydroxyNP). ^{1}H NMR ($CDCl_3$): λ ppm = 7.69–7.08 (m, 6H); 4.98 (q, 1H, *J* = 6.4 Hz); 3.73 (s, 3H); 2.03 (s, 1H), 1.51 (d, 3H, *J* = 6.4 Hz). MS: *m*/*z*

(uma) = 202; 220 $(M+NH_4)^+$, 237 $(M+N_2H_7)^+$. UV: λ_{max} (diethyl oxyde) = 232, 264, 272, 318 and 334 nm; λ_{max} (ethanol) = 232, 262, 272, 318 and 332 nm; λ_{max} (phosphate buffer) = 226, 264, 276, 314 and 332 nm.

2.2.3.3. 2-Acetyl-6-methoxynaphtalene (AcetylNP). ^{1}H NMR ($CDCl_3$): λ ppm = 8.33–7.08 (m, 6H); 3.89 (s, 3H); 2.64 (s, 3H). MS: *m*/*z* (uma) = 200; 201 $(M+H)^+$, 218 $(M+NH_4)^+$, 235 $(M+N_2H_7)^+$. UV: λ_{max} (diethyl oxyde) = 242, 258 and 306 nm; λ_{max} (ethanol) = 242, 260 and 310 nm; λ_{max} (phosphate buffer) = 242, 260 and 312 nm.

2.3. Photosensitization experiments, preparation of ^{32}P end-labelled oligonucleotides

Oligonucleotide **1** was radiolabelled at the 5′-end using standard procedures. Typically, 15 μCi of [γ^{32}P] ATP and 5 pmol of oligonucleotide were added to the Ready-to-Go T4 Polynucleotide Kinase. The mixture was incubated 30 min at 37 °C and the reaction stopped by addition of 5 μL of 250 mM ethylenediamine tetraacetic acid. Then, to remove free [γ^{32}P] ATP, the reaction mixture was purified using G-25 Microspin columns. Double-stranded DNA was obtained by mixing the 5′-end-labelled oligonucleotide with the same amounts of its unlabeled complementary strand, heating 10 min at 70 °C and cooling slowly to room temperature.

2.4. Frank and alkali-labile lesions

All the solutions were prepared in 5 mM phosphate buffer with 10 mM NaCl, pH 7.4. Samples containing 5 μL of radiolabelled oligonucleotide (40,000 cpm/μL), 10 μL of drug (40 μM), 10 μL of unlabeled double-strand oligonucleotides **1**–**2** (20 μM) and 25 μL phosphate buffer solution were irradiated at 25 °C using a xenon lamp (Muller 450 W) equipped with a long pass filter $\lambda > 320$ nm (Oriel, WG-320). The samples received ca. 11 mW cm^2 in UVA. After irradiation, samples used for the detection of frank breaks were lyophilized. For the detection of alkali-labile sites, 20 μL of freshly prepared 1 M piperidine was added and the samples were heated for 30 min at 90 °C. Piperidine was then removed by lyophilization.

2.5. Electrophoresis analysis

Before electrophoresis, the samples were resuspended in 10 μL of formamide sequencing buffer. Frank breaks and alkali-sensitive lesions were assayed by 20% denaturing (7 M urea) polyacrylamide gel electrophoresis and visualized after exposure of autoradiogram overnight at −70 °C. G markers were prepared as described [21].

2.6. Fluorescence experiments

Emission and excitation spectra were recorded with a Quanta Master (PTI) spectrofluorometer (London, ON, Canada) equipped with a xenon source and a Hammamatsu R928 photomultiplier tube. The excitation and emission monochromator pass bands were 4 nm. The emission intensity was detected at right angles by exciting solutions having an absorbance of about 0.05 in a 10 mm quartz cell at the selected excitation wavelength. All spectra were recorded in the photo-counting mode and corrected with curves given by the manufacturer. The cell was thermostated at 4 °C by water circulation. For the estimation of the fluorescence quantum yields of products in different solvents, quinine bisulfate in 1 N sulfuric acid was used as the standard ($\Phi_F = 0.55$). Fluorescence lifetimes were obtained by means of a Time Master apparatus (N_2/He 30/70 lamp, 4 ns full width at half maximum) using the strobe technique.

2.7. Phosphorescence experiments

Emission spectra were obtained on a Perkin–Elmer LS-50B spectrofluorometer equipped with a xenon source (flash duration 8 μs) and a Hamamatsu R928 photomultiplier tube with the low-temperature accessory. The apparatus was operated in time-resolved mode with a delay time of 0.15 ms. Excitation and emission monochromator pass bands of 4 nm were used. The sample was introduced in a capillary tube (2 mm diameter) and cooled to 77 K in a liquid nitrogen bath. Dry nitrogen circulation in the cell compartment avoided water condensation on the cell walls. The emission was obtained by exciting the samples at 340, 314, and 330 nm for KP, TP, and NP respectively, in ethanol, using an absorbance of about 0.05 in a 10 mm cell. Phosphorescence lifetimes (τ) were obtained by time-resolved detection of the emission intensity at the maximum-emission wavelength. The emission decay curves were fitted to the equation $I(t) = I_0 \exp(-t/\tau)$ using a non-linear least squares minimization algorithm. High correlations (0.999) were obtained in all cases.

2.8. Electrochemistry

Electrochemical measurements were carried out at room temperature with an Autolab 20 potentiostat (EcoChemie). The electrochemical cell (10 mL) was a conventional one with three electrodes: working electrodes, Platinum Pt (disk diameter: 0.5 mm for cyclic voltammetry and 2 mm for steady state experiments) for oxidation phenomena, or glassy carbon (disk diameter: 10 μm PAR for cyclic voltammetry and 3 mm for steady state experiments) for reduction phenomena; counter electrode, Pt wire; and reference electrode, double junction SCE. Cyclic voltammetry and steady state experiments were performed in acetonitrile (HPLC grade, SDS)/Bu_4NPF_6 0.1 M (Fluka, electrochemical grade) under argon atmosphere. Potential scan speed varies from 0.1 to 400 V s^{-1} during cyclic voltammetry, and rotation electrode varies from 500 to 3000 rpm during steady state experiments. The reduction potentials evaluated in acetonitrile have been then translated in phosphate buffer by adding 0.42 V/SCE, deduced from the difference between the reduction potential values of benzophenone determined into these two solvents [22].

3. Results and discussion

3.1. Photosensitization of alkali-labile lesions induced by KP, TP and NP

The efficiency of DNA alkali-labile lesions photoinduced by parent drugs was examined by gel sequencing experiments using ^{32}P-end-labelled 20 mer 5′-d[$T_1G_2A_3T_4C_5G_6G_7T_8G_9C_{10}G_{11}T_{12}C_{13}T_{14}G_{15}A_{16}G_{17}A_{18}C_{19}T_{20}$]-3′ oligonucleotide **1**. Oligonucleotide **1** presents several guanines under different sequences in order to study the involvement of an electron transfer from a guanine base to the excited photosensitizer; guanine is the easiest site for oxidation in DNA, due to its low oxidation potential [23,24].

A phosphate buffered solution containing a mixture of drug and oligonucleotide duplex was UVA-irradiated by a xenon lamp with a long pass filter at $\lambda > 320$ nm. After irradiation, samples were placed on a polyacrylamide gel, with or without hot piperidine treatment in order to visualize alkali-labile or spontaneous damage respectively.

The autoradiogram recorded after photolysis of double stranded DNA-NSAIDs mixtures is shown in Fig. 1.

No cleavage was observed on double-stranded oligonucleotide, before or after piperidine treatment (lines B), when DNA solution was irradiated alone. In presence of KP, only a very low level of direct chain break on polynucleotide backbone was detected (line C_2). On the other hand, the production of piperidine alkali-labile

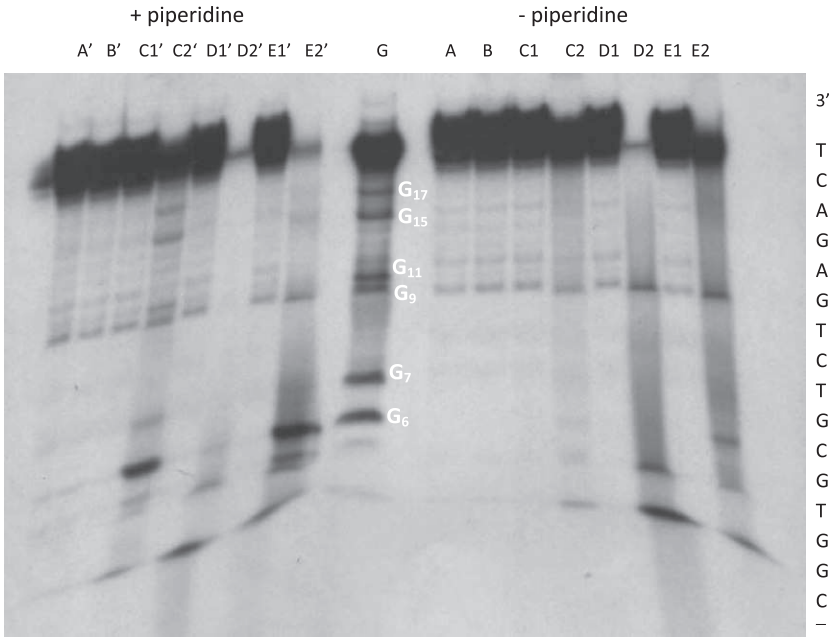

Fig. 1. Double-strand oligonucleotide (20 μM base pairs) non irradiated (line A), irradiated alone 2 h at $\lambda > 320$ nm (line B), non irradiated in the presence of 40 μM of KP, TP or NP (lines C_1, D_1 and E_1 respectively) or irradiated in the presence of 40 μM of KP, TP or NP, 2 h at $\lambda > 320$ nm (lines C_2, D_2 and E_2 respectively). Maxam and Gilbert G marker (line G).

sites essentially at 5′G of a GG step has been evidenced (line C'_2) after piperidine treatment, by comparing the cleavage pattern with the Maxam Gilbert G-marker (line G). It is now well known that the presence of a GG site in DNA will act as a "potential trap" [24,25]. This specific oxidation is relevant of a mechanism involving an electron transfer from the guanine to the excited photosensitizer, in agreement with the literature [8].

When DNA is UVA-irradiated in presence of TP (Fig. 1) a high level of direct strand breaks was observed without piperidine treatment (line D_2) relevant of a Type I radical mechanism, in agreement with the literature [13]. Moreover, no selective cleavage at 5′ of the -GG- site was observed after alkali-labile treatment, showing the absence of implication of an electron transfer mechanism in these oxidative processes (line D'_2).

When DNA is UVA-irradiated in presence of NP (Fig. 1), spontaneous strand breaks were observed without hot piperidine treatment (line E_2), as reported previously [6,11]. Selective cleavage at the guanine in 5′ of -GG- site after alkali-labile treatment (line E'_2) showed a high efficiency of an electron transfer mechanism.

For KP and NP, other guanine residues were also altered but with lower efficiency suggesting probably the involvement of singlet oxygen. However, the DNA cleavage efficiency being in accordance with the calculated lowest ionization potentials of stacked nucleobase models [24,25], this pattern confirms for these two drugs mainly the intervention of a one electron transfer oxidation in these processes, singlet oxygen intervening probably only in lesser proportion.

However, it has been previously demonstrated that these three NSAIDs are unstable under irradiation and their photolysis leads to three major photoproducts, the ethyl, hydroxyethyl and acetyl derivates, which may be at the origin of these photosensitizing reactions.

3.2. Photosensitization of alkali-labile lesions induced by KP, TP and NP photoproducts

Photosensitizing properties of each NSAIDs photoproduct towards DNA were investigated to conclude about their potential role in photodamage on guanine sites by one electron transfer oxidation. The results obtained are shown in Figs. 2–4.

When DNA is irradiated in presence of each KP photoproducts (Fig. 2), the production of piperidine alkali-labile sites essentially at 5′-G of GG steps (lines D'_2, E'_2, F'_2) has been observed, suggesting an efficient electron transfer mechanism next to a minor involvement of singlet oxygen, as for the parent drug. A similar efficiency in electron transfer mechanism is observed for the photoproducts and the parent drug.

When DNA is irradiated in presence of each TP photoproducts (Fig. 3) and without piperidine treatment, important level of spontaneous strand breaks was observed (lines D_2, E_2, F_2), as for the parent drug. On the other hand, contrary to the parent drug, a low amount of alkali-labile lesions only at the guanine residue at 5′ of -GG- site is observed after hot piperidine treatment for hydroxyTP and ethylTP (lines E'_2, F'_2 respectively) indicating a contribution of the electron transfer mechanism in these photosensitized oxidation processes. A similar efficiency was observed for these two photoproducts.

When DNA is irradiated in presence of each NP photoproducts and without alkali-labile treatment (Fig. 4), direct strand breaks were observed for acetylNP and hydroxyNP (lines D_2, E_2). After piperidine treatment, the damage level was important, especially on guanine at 5′ of the -GG- step, for acetylNP, hydroxyNP and to a lower extent for ethylNP, suggesting the intervention of an efficient electron transfer mechanism in these processes (lines D'_2, E'_2, F'_2 respectively), next to a minor involvement of singlet oxygen, as for the parent drug.

3.3. Emission spectra

Emission experiments were carried out in order to study the excited-state properties of these compounds, at the origin of the photoinduced electron transfer. The photophysical properties of the NSAIDs photoproducts were investigated and compared with whose of those parent drug. Fluorescence spectra were recorded at 4 °C in ethanol, phosphate buffer and diethyl oxide.

KP family presented no (for KP and AcetylKP) or a weak (for HydroxyKP and EthylKP) fluorescence emission in ethanol.

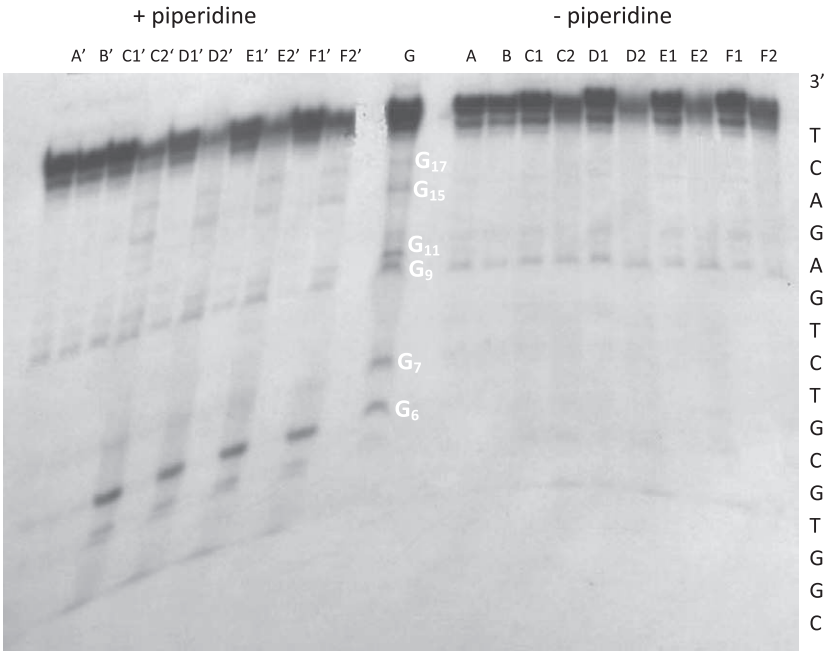

Fig. 2. Double-strand oligonucleotide non irradiated (line A), irradiated alone 2 h at $\lambda > 320$ nm (line B), non irradiated in the presence of 40 μM of KP, AcetylKP, HydroxyKP or EthylKP (lines C_1, D_1, E_1 and F_1 respectively) or irradiated in the presence of 40 μM of KP, AcetylKP, HydroxyKP or EthylKP (lines C_2, D_2, E_2 and F_2 respectively). Maxam and Gilbert G marker (line G).

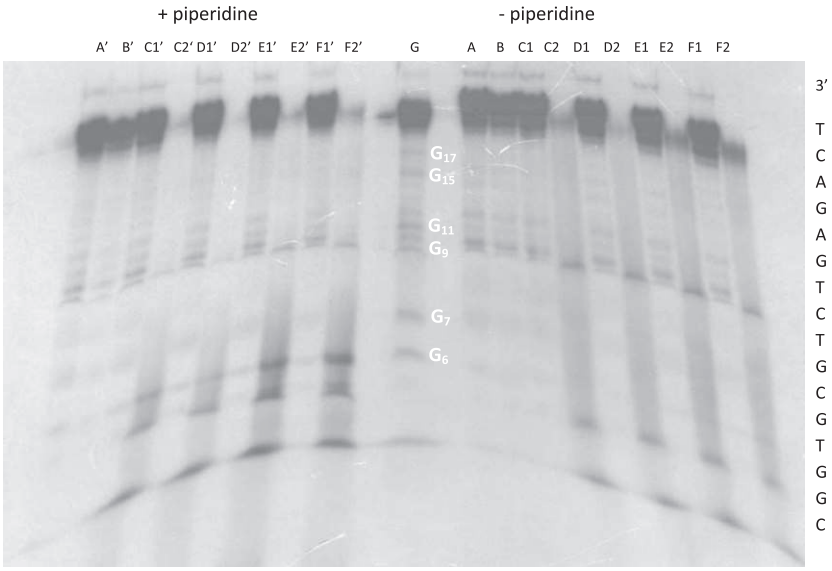

Fig. 3. Double–strand oligonucleotide non irradiated (line A), irradiated alone 2 h at $\lambda > 320$ nm (line B), non irradiated in the presence of 40 μM of TP, AcetylTP, HydroxyTP or EthylTP (lines C_1, D_1, E_1 and F_1 respectively) or irradiated in the presence of 40 μM of TP, AcetylTP, HydroxyTP or EthylTP (lines C_2, D_2, E_2 and F_2 respectively). Maxam and Gilbert G marker (line G).

However, in diethyl oxide, a very weak fluorescence signal was able to be measured for AcetylKP.

No fluorescence signal was detected for TP and its photoproducts in ethanol. In phosphate buffer and diethyl oxide, only a very low fluorescence emission was observed, making any assignment difficult.

NP and its photoproducts displayed a strong fluorescence emission by comparison with the others compounds.

Singlet excited state energies were calculated from the intersection of the normalized excitation and emission spectra. Fluorescence quantum yields were also determined for KP, NP and their corresponding photoproducts. All results are reported in Table 1.

Although the evolution of fluorescence quantum yield does not match exactly the intersystem crossing quantum yield (Φ_{ISC}), it presents a correct reflection axis. The differences in fluorescence emission can be partially explained in terms of Φ_{ISC}, if we neglect nonradiative processes. Taking in mind these considerations, KP and TP families had probably a more efficient Φ_{ISC} than NP family, suggesting for these two families a photoreactivity initiated by a

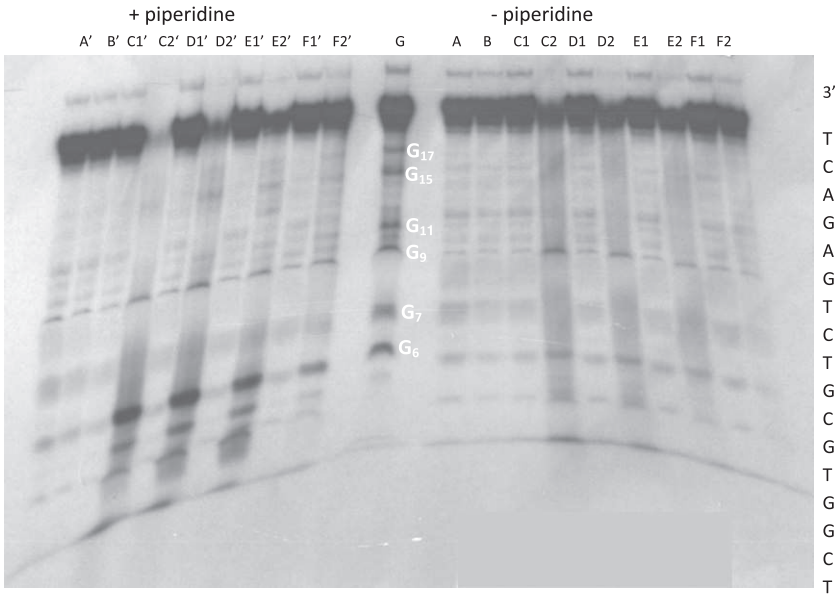

Fig. 4. Double-strand oligonucleotide non irradiated (line A), irradiated alone 2 h at $\lambda > 320$ nm (line B), non irradiated in the presence of 40 μM of NP, AcetylNP, HydroxyNP or EthylNP (lines C_1, D_1, E_1 and F_1 respectively) or irradiated in the presence of 40 μM of NP, AcetylNP, HydroxyNP or EthylNP (lines C_2, D_2, E_2 and F_2 respectively). Maxam and Gilbert G marker (line G).

Table 1
Photophysical properties of singlet and triplet excited states of KP, TP, NP and their major photoproducts.

	$\Delta_S E_{0-0}$ (kJ mol^{-1})	Φ_F	Φ_{ISC}	$\Delta_T E_{0-0}$ (kJ mol^{-1})
KP	321[4]	–	1[4]	289[b]
Acetyl KP	382[a]	–[b]	–	289[b]
Hydroxy KP	378[b]	0.048[b]	–	289[b]
Ethyl KP	372[b]	0.013[b]	–	289[b]
TP	338[4]	–[b]	0.9[4]	242[b]
Acetyl TP	–[b]	–[b]	–	221[b]
Hydroxy TP	–[b]	–[b]	–	242[b]
Ethyl TP	–[b]	–[b]	–	238[b]
NP	358[b]	0.13[b]	0.28[4]	259[b]
Acetyl NP	376[b]	0.191[b]	–	288[b]
Hydroxy NP	356[b]	0.377[b]	–	259[b]
Ethyl NP	356[b]	0.349[b]	–	238[b]

E_S determined from emission spectra at 4 °C; for HydroxyKP, EthylKP and Acetyl NP: λ_{exc} = 300 nm, for HydroxyNP and EthylNP: λ_{exc} = 330 nm.
E_T determined from low-temperature (77 K) phosphorescence emission spectra in an ethanol glass; for KP family: λ_{exc} = 340 nm, for TP family: λ_{exc} = 314 nm, for NP family: λ_{exc} = 330 nm.
[a] Ether.
[b] Ethanol.

triplet excited-state rather than by the singlet excited-state. To obtain further information about the excited state photoreactivity, phosphorescence experiments were carried out.

Phosphorescence emission spectra were recorded at 77 K in ethanol. All compounds displayed a phosphorescence emission. The lowest triplet excited-state energies were evaluated from the 0–0 bands of the emission spectra. The main photophysical parameters are summarized in Table 1. Triplet state energies of KP, TP and NP are in agreement with previous data [4,26]. For the KP family, the three major photoproducts have triplet state energies similar to that the parent drug. Concerning TP and NP photoproducts, triplet state energies are similar or different from the parent drug ones.

As a conclusion, these results suggested that for KP and TP family, the photoinduced electron transfer was initiated by the triplet excited-state whereas for NP family, photooxidative reactivity from their triplet excited-state or from their singlet excited-state has to be considered.

3.4. Electrochemical behavior

To investigate the electron acceptor properties of these compounds, electrochemical experiments were performed. The photosensibilization mechanism leading to the oxidation of guanine nucleobase involves the $PS^*/PS^{\cdot -}$ redox couple: radical cation formation *via* electron transfer to the excited state of the photosensitizer.

Only the cathodic behavior of the photosensitizers is described. Electrochemical data were obtained in acetonitrile because of its large electroactivity domain. The potentials were then calculated for water, taking as references the reduction potentials of acetophenone in the two media [27]. Under stationary conditions (rotating electrode), half wave potentials $E_{1/2}$ and diffusion currents were measured; diffusion coefficients were calculated according to the Levich equation [28]. Peak potentials Ep and currents Ip on the forward and backward scans were measured by cyclic voltammetry: the peak separation $\Delta Ep = |Ep_{backward} - Ep_{forward|}/\log v$ and the peak ratio $RIp = Ip_{backward}/Ip_{forward}$ were calculated as a function of potential scan speed (v). Analysis of these parameters provided (i) the electron transfer constant k° from $\Delta Ep = f(\log v)$ [28,29]; (ii) the reversibility of the electron transfer or the stability of the radical anion $PS^{\cdot -}$ from $RIp = f(v)$ [28,30].

Using a glassy carbon electrode (Cv), the reversibility of the reduction process reflects the stability of the reduction product (Fig. 5, Table 2). During the forward scan, a reduction peak was observed related to the formation of the radical anion $PS^{\cdot -}$. During the backward scan, the oxidation of the radical anion is more or less observed depending on the potential scan speed and the relative stability of the radical anion $PS^{\cdot -}$. The electrochemical system is represented by an EC scheme (electrochemical transfer (E) followed by a chemical reaction (C)):

$$PS + e^- \underset{k^\circ}{\overset{E}{\rightleftharpoons}} PS^{\cdot -} \xrightarrow[k]{C} \text{product}$$

When the potential scan speed is increased, the peak ratio RIp increases because of the freezing of the chemical step and the peak separation ΔEp increases, showing a kinetic control of the electron

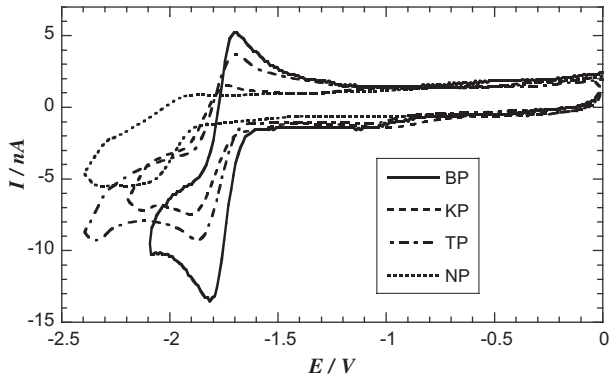

Fig. 5. Reduction of BP, KP, TP et NP: cyclic voltammograms at a glassy carbon electrode in CH_3CN/Bu_4NPF_6 0.1 M; [PS] = 1 mM ; potential scan speed 1 V s^{-1}.

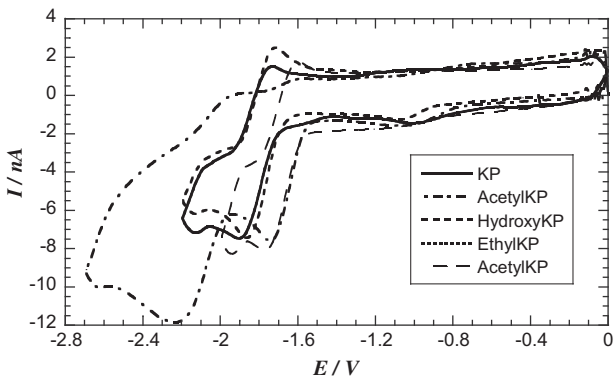

Fig. 6. KP photoproducts: cyclic voltammograms at a glassy carbon electrode in CH_3CN/Bu_4NPF_6 0.1 M; [PS] = 1 mM; potential scan speed 1 V s^{-1}. For AcetylKP, the first voltammogram is centered on the first electrochemical system, whereas the second one shows the two electrochemical systems.

transfer and leading to the calculation of the electron transfer constant k°. Peak currents (Ip) are proportional to the square root of the potential scan speed, as for a diffusion controlled process, in agreement with the Randles–Sevcik equation [28].

As the electrochemical system of benzophenone (BP) corresponds to the reduction of the carbonyl function [22,31], $BP + e^- \rightarrow BP^{\cdot -}$, the reduction processes for KP and TP can be attributed to this same C=O function. For NP, the reduction peak observed corresponds to naphthalene moiety reduction, in agreement with the literature [32–34].

The photoproduct voltammograms (Fig. 6) are similar to those of the parent drugs except for acetyl derivatives in which reduction of an additional C=O group has to be taken into account. As this function is terminal, its reduction should occur at a more cathodic potential than the one of the central carbonyl group of KP and TP.

Whatever the compound, an increase of potential scan speed modifies the voltammograms patterns: (i) the peak ratio RIp increases and tends towards 1, showing that the system becomes fully reversible, and (ii) the peak separation ΔEp increases, showing the kinetic control of the electron transfer. Analysis of these parameters as a function of potential scan speed led us to determine the electron transfer constant. The compounds present k° values between 0.007 and 0.09 cm s^{-1}, such as $Fe(CN)_6^{3-}/Fe(CN)_6^{4-}$ (Table 2). Moreover, analysis of the peak ratio RIp allows us to evaluate the stability of the radical anion $PS^{\cdot -}$ by considering a simple EC mechanism above written [30]. The radical anion stability can be evaluated by calculating its half-life $t_{1/2} = \mathrm{Ln}\,2/k$ (Table 2): radical anions of the NP family are the most unstable.

3.5. Correlation between electron transfer mechanism efficiency and PS physicochemical properties

Differences in the photosensitization properties of the investigated compounds can be correlated to their photophysical and electrochemical characteristics. Indeed, the photooxidation process, which involves an electron transfer from the nucleobase to the excited state of the photosensitizer, may be summarized by the following sequence, previously proposed [27]:

Light absorption	$PS + h\nu$	$\rightarrow$	PS^*	(1)
Deactivation	PS^*	$\rightarrow$	PS	(2)
Photooxidation	$PS^{\cdot -} + G$	$\rightarrow$	$PS^{\cdot -} + G^{\cdot +}$	(3)
Back reaction	$PS^{\cdot -} + G^{\cdot +}$	$\rightarrow$	$PS + G$	(4)
Stability of $PS^{\cdot -}$	$PS^{\cdot -}$	$\rightarrow$	products	(5)
Stability of $G^{\cdot -}$	$G^{\cdot +}$	$\rightarrow$	products	(6)

The energy diagram of the photosensitized electron transfer mechanism is represented on Scheme 2 with the protocol followed for the determination of $\Delta_r G°$. Photophysical measurements gave the values of $\Delta_T E_{0-0}$ and $\Delta_S E_{0-0}$. Cyclic voltammetry measure-

Table 2
Reduction parameters of parent drugs and their photoproducts in CH_3CN/Bu_4NPF_6 0.1 M, glassy carbon electrode (r = 10 μm). Thermodynamic and kinetic parameters for KP, TP and NP photooxidative processes.

	Redox potential E° (V/ECS)	Electron transfer rate k°_{red} (cm s^{-1})	$PS^{\cdot -}$ Lifetime $t_{½}$ (s)	ΔrG° (kJ mol^{-1}) (triplet)	ΔrG° (kJ mol^{-1}) (singlet)
KP	−1.82	0.09	~0.66	−98	
AcetylKP	−1.69	0.04	~0.56	−111	
	−2.02	0.02	~0.14	−78	
HydroxyKP	−1.80	0.07	~0.75	−100	
EthylKP	−1.80	0.08	~0.79	−99	
TP	−1.78	0.08	~1.52	−54	
AcetylTP	−1.23	0.08	~1.31	−86	
	−1.68	0.05	~3.0	−43	
HydroxyTP	−1.73	0.04	~0.05	−60	
EthylTP	−1.72	0.06	~0.25	−57	
NP	−2.04	0.04	~0.19	−47	−146
AcetylNP	−1.99	0.05	~0.10	−80	−168
	−2.66	0.01	~0.22	−15	−103
HydroxyNP	−2.63	0.05	~0.08	+10	−87
EthylNP	−2.49	0.007	~0.26	+18	−100

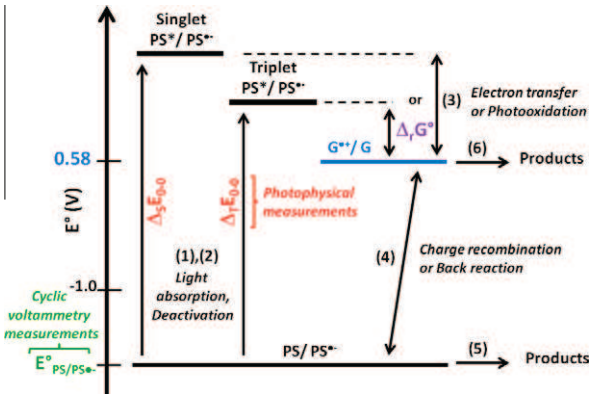

Scheme 2. Energy diagram of photosensitized electron transfer mechanism.

ments gave the stability of $PS^{\cdot-}$ (reaction 5) and the redox potential $E°(PS/PS^{\cdot-})$ in the dark which was translated to the phosphate buffer

Photodamage effects are related to reactions (1–3). The Gibbs free energy for photo-induced electron transfer is given [20]:

$$\Delta_r G° = 96.5[E°(G^{\cdot+}/G) - E°(PS/PS^{\cdot-})] - \Delta E_{0-0}\left(\text{kJ mol}^{-1}\right)$$

where ΔE_{0-0} is the energy of the PS excited state ($\Delta_T E_{0-0}$ for triplet state or $\Delta_S E_{0-0}$ for singlet state); $E°(G^{\cdot+}/G) = 0.58$ V/SCE is the calculated oxidation potential of the guanine for the 5′-G of the -GG- site [24,25] and $E°(PS/PS^{\cdot-})$ is the reduction potential of PS in phosphate buffer.

From a thermodynamic point of view, photooxidation is possible if the free energy $\Delta_r G°$ is negative. But, the observed differences in photosensitizing properties of the compounds are not related to thermodynamic features only. In the above scheme, the back reaction (4) which is exergonic, attenuates the effects of photooxidation and is in part controlled by the stability of $PS^{\cdot-}$ and $G^{\cdot+}$. Taking into account that reaction (6), product formation from $G^{\cdot+}$, does not depend on the nature of the PS, the relative efficiency of electron transfer may be related to reaction (5). Indeed, the photoactivity and the stability of $PS^{\cdot-}$ are associated: if $PS^{\cdot-}$ is unstable, the back reaction (4) does not proceed and high photooxidative damages are obtained.

In order to calculate thermodynamic parameters, the implicated excited states have to be known. If there is no ambiguity for KP and TP families, it is not the case for NP. Indeed, KP and TP display very high intersystem-crossing quantum yields (1 and 0.9 respectively for KP and TP) [4,35]. Therefore, reactivity from their triplet state can be assumed. The same is true for KP and TP photoproducts. Their very weak or the absence of fluorescence emission suggests, as for the parent drugs, involvement of their triplet excited states. On the other hand, for NP and its photoproducts, reactivity from their triplet state or from their singlet state have to be considered since Φ_{ISC} for NP is 0.28 [4] and that an important Φ_F is observed as well for NP as for its photoproducts.

The changes in free energy for the electron transfer were found exergonic between compounds of KP family and a guanine at 5′ at -GG- site, the same behavior is observed for compounds of TP family. As to NP family, for which the implicated excited state is unknown, photooxidation is thermodynamically possible for NP and AcetylNP from triplet and singlet state, even if the electron transfer is more favorable in the case of the singlet excited state. For HydroxyNP and EthylNP, reaction is possible only from their singlet excited state. Therefore, it seems obvious that NP and their photoproducts react more easily from their singlet than from their triplet excited state.

Among the three drugs, NP is more efficient than KP and TP in producing oxidative damages by electron transfer. It can be justified:

- from a thermodynamic point of view, $\Delta_r G°$ of NP is the most exergonic (-146 kJ mol^{-1}) while $\Delta_r G°$ of TP is the less exergonic;
- from a kinetic point of view, $NP^{\cdot-}$ is the most unstable and back-reaction (4) is prevented leading to increased damages; in contrast, $TP^{\cdot-}$ is the most stable, back-reaction (4) is efficient and TP is not involved in this oxidative process. It can be noticed that NP presents the lowest value of electron transfer constant k°; it would show that k° is not a major factor by contrast to $t_{1/2}$.

Similar correlations are highlighted with the photoproducts which appeared as electron transfer photosensitizers:

- Concerning the TP family that showed a weak oxidative activity by electron transfer, HydroxyTP and EthylTP present comparable efficiencies and AcetylTP is the less efficient photosensitizer. $\Delta_r G°$ free energies values cannot contribute to the understanding of these differences of efficiency, reactions are most probably under kinetic control. Indeed, $t_{1/2}$ of HydroxyTP and EthylTP are weaker than that of AcetylTP, explaining the different efficiencies.
- In the case of KP photoproducts, no significant differences in efficiency were observed. Indeed, $\Delta_r G°$ values are close as well as $t_{1/2}$; the photodamages are equivalent.
- Concerning the NP family, AcetylNP appears to be the most efficient photosensitizer, with a highly negative $\Delta_r G°$ value (-168 kJ mol^{-1}) and its radical anion $AcetylNP^{\cdot-}$ is unstable. The $\Delta_r G°$ values for EthylNP and HydroxyNP are of the same order of magnitude and the radical anion $HydroxyNP^{\cdot-}$ is less stable than $EthylNP^{\cdot-}$: the back reaction (4) explains the different photoefficiencies, HydroxyNP is the most efficient.

4. Conclusions

This photoredox and photobiological study proved the ability of three NSAIDs, Ketoprofen, Tiaprofenic acid and Naproxen and their photoproducts, to induce DNA photooxidation *via* an electron transfer mechanism and bore out the direct implication of photoproducts in the photosensitizing reactions. Indeed, the three main photoproducts of these drugs (Acetyl, Hydroxyethyl and Ethyl derivatives) were involved in the photooxidative damages. Concerning KP and NP family, electron transfer is the predominant mechanism, whereas in the case of TP family, it seems to be a minor process. Moreover, spectroscopies and cyclic voltammetry allowed us to correlate photoredox properties of these compounds with photobiological properties in term of electron transfer. From a general point of view, this work underlines the necessity to consider the photochemical properties of any chemicals and the photophysical properties of their photoproducts before their commercial uses.

References

[1] B. Ljunggren, Propionic acid-derivated are phototoxic in vitro, Photodermatol 2 (1985) 3–9.
[2] I.E. Kochevar, Phototoxicity of non-steroidal antiinflammatory drugs: coincidence or specific mechanism, Arch. Dermatol. 125 (1989) 824–826.
[3] G. Condorelli, G. De Guidi, S. Giuffrida, L.L. Costanzo, Photosensitizing action of nonsteroidal antiinflammatory drugs on cell membranes and design of protective system, Coord. Chem. Rev. 125 (1993) 115–128.
[4] F. Bosca, M. Luisa Marin, M.A. Miranda, Photoreactivity of the nonsteroidal anti-inflammatory 2-arylpropionic acids with photosensitizing side effects, Photochem. Photobiol. 74 (2001) 637–655.

[5] S. Liu, H. Mizu, H. Yamauchi, Photoinflammatory responses to UV-irradiated ketoprofen mediated by the induction of ROS generation, enhancement of cyclogenase-2 expression, and regulation of multiple signaling pathways, Free Radical Biol. Med. 48 (2010) 772–780.
[6] N. Chouini-Lalanne, M. Defais, N. Paillous, Nonsteroidal antiinflammatory drug-photosensitized formation of pyrimidine dimer in DNA, Biochem. Pharmacol. 55 (1998) 441–446.
[7] M.C. Marguery, N. Chouini-Lalanne, J.C. Ader, N. Paillous, Comparison of the DNA damage photoinduced by fenofibrate and ketoprofen, two phototoxic drugs of parent structure, Photochem. Photobiol. 68 (1998) 679–684.
[8] V. Lhiaubet, N. Paillous, N. Chouini-Lalanne, Comparison of DNA damage photoinduced by ketoprofen, fenofibric acid and benzophenone via electron and energy transfer, Photochem. Photobiol. 74 (2001) 670–678.
[9] J. Cadet, T. Douki, J.L. Ravanant, Oxidatively generated base damage to cellular DNA, Free Radical Biol. Med. 49 (2010) 9–21.
[10] C.S. Foote, Definition of type I and type II photosensitized oxidation, Photochem. Photobiol. 54 (1991) 659.
[11] T. Artuso, J. Bernadou, B. Meunier, J. Piette, N. Paillous, Mechanism of DNA cleavage mediated by photoexcited non-steroidal anti-inflammatory drugs, Photochem. Photobiol. 54 (1991) 205–213.
[12] G. De Guidi, S. Giuffrida, G. Condorelli, L.L. Costanzo, P. Miano, S. Sortino, Molecular mechanism of drug photosensitization. IX: effect of inorganic ions on DNA cleavage photosensitized by naproxen, Photochem. Photobiol. 63 (1996) 455–462.
[13] C. Agapakis-Causse, F. Bosca, J.V. Castell, D. Hernandez, M.L. Marin, L. Marrot, M.A. Miranda, Tiaprofenic acid-photosensitized damage to nucleic acids: a mechanistic study using complementary in vitro approaches, Photochem. Photobiol. 71 (2000) 499–505.
[14] F. Bosca, M.A. Miranda, G. Carganico, D. Mauleon, Photochemical and photobiological properties of ketoprofen associated with the benzophenone chromophore, Photochem. Photobiol. 60 (1994) 96–101.
[15] F. Bosca, M.A. Miranda, F. Vargas, Photochemistry of tiaprofenic acid, a non-steroidal anti-inflammatory drug with phototoxic side effects, J. Pharm. Sci. 81 (1992) 181–182.
[16] D.E. Moore, P.P. Chappuis, A comparative study of the photochemistry of the non-steroidal anti-inflammatory drugs, naproxen, benoxaprofen and indomethacin, Photochem. Photobiol. 47 (1988) 173–180.
[17] A.L. Vinette, J.P. McNamee, V. Bellier, J.R.N. McLean, J.C. Scaiano, Prompt and delayed nonsteroidal anti-inflammatory drug-photoinduced DNA damage in peripheral blood mononuclear cells measured with the comet assay, Photochem. Photobiol. 77 (2003) 390–396.
[18] V. Lhiaubet-Vallet, J. Trzcionka, S. Encinas, M.A. Miranda, N. Chouini-Lalanne, The triplet state of a N-phenylphthalimidine with high intersystem crossing efficiency: characterization by transient absorption spectroscopy and DNA sensitization properties, J. Phys. Chem. B 108 (2004) 14148–14153.
[19] J. Trzcionka, A. Noirot, P.L. Fabre, N. Chouini-Lalanne, Comparative study of the photophysical properties of indoprofen photoproducts in relation with their DNA photosensitizing properties, Photochem. Photobiol. Sci. 4 (2005) 298–303.
[20] D. Rehm, D.A. Weller, Kinetics of fluorescence quenching by electron an H-atom transfer, Isr. J. Chem. 8 (1970) 259–271.
[21] A.M. Maxam, W. Gilbert, Sequencing end-labeled DNA with base specific chemical cleavages, Methods Enzymol. 65 (1980) 499–559.
[22] K.R. Walczyk, G.S. Popkirov, R.N. Schindler, Investigation of the redox couple benzophenone/benzophenone anion radical in acetonitrile and N,N-dimethylformamide by electrochemical and spectroelectrochemical methods, Ber. Bunsen-Geset. 99 (1995) 1028–1036.
[23] Y. Yoshioka, Y. Kitagawa, Y. Takano, K. Yamaguchi, T. Nakamura, I. Saito, Experimental and theotitical studies on the selectivity of GGG triplets toward one-electron oxidation in B-form DNA, J. Am. Chem. Soc. 121 (1999) 8712–8719.
[24] C.J. Burrows, J.G. Muller, Oxidative nucleobase modification leading to strand scission, Chem. Rev. 98 (1998) 1109–1151.
[25] H. Sugiyama, I. Saito, Theorical studies of -GG- specific photocleavage of DNA via electron transfer: significant lowering of ionization potential and 5′-localization of HOMO of stacked GG bases in B-form DNA, J. Am. Chem. Soc. 118 (1996) 7063–7068.
[26] L.J. Martinez, J.C. Scaiano, Characterization of the transient intermediates generated from the photoexcitation of nabumetone: a comparison with naproxen, Photochem. Photobiol. 68 (1998) 646–651.
[27] P.L. Fabre, L. Latapie, A. Noirot, N. Chouini-Lalanne, Correlation of cyclic voltammetry behaviour and photooxifative properties of indoprofen and its photoproducts, Electrochim. Acta 52 (2006) 102–107.
[28] Southampton Electrochemistry Group, Instrumental method in electrochemistry. Chichester GB: Ellis Horwood Ltd.; 1985.
[29] R.S. Nicholson, I. Shain, Theory and application of cyclic voltammetry for measurement of electrode reaction kinetics, Anal. Chem. 37 (1965) 1351–1355.
[30] R.S. Nicholson, I. Shain, Theory of stationary electrode polarography. Single scan and cyclic methods applied to reversible, irreversible, and kinetic systems, Anal. Chem. 36 (1964) 706–723.
[31] P.J. Wagner, R.J. Truman, A.E. Puchalski, R. Wake, Extent of charge transfer in the photoreduction of phenyl ketones by alkylbenzenes, J. Am. Chem. Soc. 108 (1986) 7727–7738.
[32] J.B. Ketter, R.M. Wightman, Tuning emissive states in electrogenerated chemiluminescence. Behavior of electrogenerated bases in room-temperature ionic liquids, J. Am. Chem. Soc. 126 (2004) 10183–10189.
[33] S. O'Toole, S. Pentlavalli, A.P. Doherty, Behavior of electrogenerated bases in room-temperature ionic liquids, J. Phys. Chem. B. 111 (2007) 9281–9287.
[34] Z. Guo, X. Jiang, X. Lin, An integrated dual ultramicroelectrode with lower solution resistance applied in ultrafast cyclic voltammetry, Anal. Sci. 21 (2005) 101–105.
[35] S. Encinas, M.A. Miranda, M. Giancarlo, S. Monti, Triplet photoreactivity of the diaryl ketone tiaprofenic acid and its decarboxylated photoproduct. Photobiological implications, Photochem. Photobiol. 67 (1998) 420–425.